해양과학기술논문집 제14권 제1호(2005)
Bull. Mar. Sci. & Tech., 14(1) : 9-16 (2005)

BULLETIN OF
RIMST MARINE SCIENCE AND TECHHNOLOGY

Experimental Study on Vortex Induced Vibrations of Highly Flexible Immersed Pipe Subjected to Top End Oscillations

H. I. Park[1]; Y. P. Hong[2]; M. Nakamura[3]; and W. Koterayama[4]

Abstract: This study reports an experimental investigation on vortex induced transverse vibrations of a highly flexible free hanging pipe. The experiment was carried out in a towing tank with a 6 m of long flexible rubber pipe, by exciting top end oscillations and measuring lateral displacements at nine points. The largest response amplitude of transverse vibrations occurs at the bottom part of the model for all excitation frequencies and amplitudes. Even though Kc numbers are different along the model length due to in-line response amplitude differences, transverse vibration frequencies are all the same along the model length. Transverse structural wave propagation is observed at the experiment and found in the measured data analysis. A transverse structural wave initiated at a particular point by vortex shedding propagates along the model length and resulting in all the response frequencies to be same.

DOI: 10.1061/(ASCE)0733-950X(2004)130:4(207)

CE Database subject headings: Laboratory tests; Vortex shedding; Flexible pipes; Transverse waves; Oscillations.

Introduction

In offshore activities, examples of free hanging marine pipes are numerous such as ocean thermal energy conversion pipes, deep sea water exploration pipes, oil exploration, and production risers during retrieval conditions. Presently, since ocean resource developments move to much deeper waters, such long slender marine structures play more important roles than before. The slender structures for ultra-deep water developments are highly flexible and exhibit very complex dynamic behaviors. Thus more exact dynamic analysis on long flexible marine structures needs to be carried out.

Vortex induced transverse vibrations of slender marine structures have been a key issue in the dynamics of slender marine structures. Even though the maximum amplitude of vortex induced vibration (VIV) is small of order of 1 diameter, it contributes to fatigue damage accumulation and increases the drag forces that may lead to operational limitations.

Vortex induced vibration of cylindrical structures has been investigated by many researchers. Sarpkaya (1979) and Griffin and Ramberg (1982) and Blevins (1990) have given comprehensive reviews of the art in respect of vortex shedding and associated vibrations of cylindrical structures. For ocean cylindrical structures, there has been some earlier research on VIV (Whitney et al. 1981). Recently, VIV of marine pipes is a matter of increasing concern as production operations move into deeper waters where structures become more flexible due to the increase of length over diameter ratio and are sensitive to VIV. In a numerical method, a VIV problem is solved by computational fluid dynamics or structural dynamics based approaches. In the former approach, an interaction between structure and fluid is analyzed by directly solving the Navier–Stokes equation (Herfjord 1999; de Oliveira et al. 2000; Schulz and Kallinderis 2000). In the latter approach, VIV is solved by using experimental hydrodynamic coefficients (Vandiver and Li 1997; Grant et al. 2000).

Numerical methods for VIV of flexible slender marine structures have many advantages but still have some uncertainties and require much computational time. So, experimental studies are being actively performed to validate numerical and/or theoretical results, to obtain some essential information for a theoretical analysis and to observe real physical phenomena. Experimental studies on slender marine structures can be performed at a model scale or a full scale. Data from full-scale measurements under realistic conditions provide very important information for understanding of VIV phenomenon of slender marine structures. A typical full-scale experiment on VIV of deepwater risers was carried out as a part of the Norwegian Deepwater Program that was formed in late 1996 by oil companies. A series of papers were published for the experimental results. Halse (2000) introduced an overview of the experimental work.

Although full-scale data provide completely representative evidence of marine structures, it is very expensive to acquire such data and very difficult to interpret it. Thus model scale tests have been more frequently carried out than full scale for slender marine structures (Lyons and Patel 1986; Sumer and Fredsoe 1988; Moe et al. 1994; Pesce and Fujarra 1999; Vikestad and Halse 2000; de Wilde and Huijsmans 2001). Recently a theoretical investigation on coupled cross-flow and in-line vibrations is also carried out for a suspended cable (Kim and Perkins 2002).

In order to cope with the requirements for ultradeep-water ocean development researches, rather a large-scale model test for a long flexible model is necessary. An experimental study on VIV

[1]Professor, Division of Ocean Development Engineering, Korea Maritime Univ., Busan 606-791, Korea. E-mail: hipark@mail.hhu.ac.kr
[2]Graduate Student, Research Institute for Applied Mechanics, Kyushu Univ., 87 Kasuga 816-8580, Japan. E-mail: yphong@riam.kyushu-u.ac.jp
[3]Assistant Professor, Research Institute for Applied Mechanics, Kyushu Univ., 87 Kasuga 816-8580, Japan. E-mail: naka@riam.kyushu-u.ac.jp
[4]Professor, Research Institute for Applied Mechanics, Kyushu Univ., 87 Kasuga 816-8580, Japan. E-mail: kotera@riam.kyushu-u.ac.jp

Note. Discussion open until December 1, 2004. Separate discussions must be submitted for individual papers. To extend the closing date by one month, a written request must be filed with the ASCE Managing Editor. The manuscript for this paper was submitted for review and possible publication on August 5, 2002; approved on November 21, 2003. This paper is part of the ***Journal of Waterway, Port, Coastal, and Ocean Engineering***, Vol. 130, No. 4, July 1, 2004. ©ASCE, ISSN 0733-950X/2004/4-207–214/$18.00.

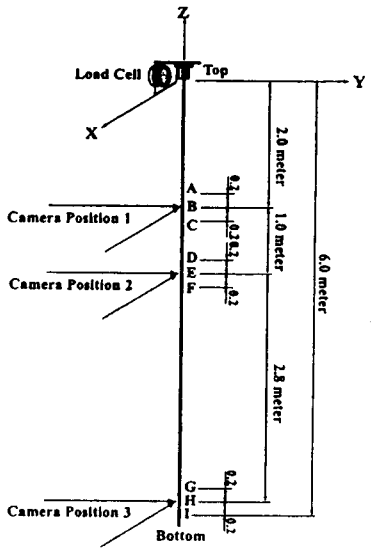

Fig. 1. Pipe model and measuring devices

of a highly flexible pipe is rare. In this research, a model test is performed for a 6 m long flexible model in towing tank 7 m deep. A rubber pipe is selected as a model for having high flexibility. The model pipe is set to be free hanging and excited by horizontal oscillations at the top end. In-line and transverse displacements are measured and analyzed to obtain its response characteristics in detail.

Test Setup

In the model test, in-line and transverse displacements of a free hanging immersed pipe model by top end oscillations are measured at several points without current (see Fig. 1). The test model is made from a rubber pipe to have high flexibility and its property is given in Table 1. In selecting the rubber pipe, any scaling of Young's modulus is not considered. The upper end is fixed to an oscillating plate and the bottom part is set to be free.

A position tracker device and underwater charge-coupled device (CCD) camera system is used to measure lateral displacements of the model. Before carrying out actual model experiments in a towing tank, static and dynamic calibration experiments are performed to obtain optical tracking and time lag errors of the position data from the tracker device. According to calibration results, the time lag error is found to be a function of exciting period (T) and can be interpolated by the following expression:

$$\Delta t_X = -2.1604\times 10^{-4}T - 0.03097$$
$$\Delta t_Z = -1.7012\times 10^{-3}T - 0.03828 \quad (1)$$

Table 1. Model Data

Material	Rubber pipe
Length	6 m
Diameter	0.02 m
Weight in air	4.758 N/m
Weight in water	1.678 N/m
Young modulus	2.33 MPa

Thus maximum position tracking errors can be calculated and are about 1.40 and 0.61 mm in horizontal and vertical directions.

Experiments are carried out in a 7 m deep towing tank that is designed and constructed for deep-water research by Research Institute for Applied Mechanics at Kyushu Univ. An electro-hydraulic actuator is mounted on the tank carriage frame. The top end of the model is fixed to the actuator plate and is excited in any prescribed horizontal displacements by control signals from a computer. The movements of the test model are measured by a position tracker device and underwater CCD camera system at three positions. One camera can track three white targets and thus measure the displacements of three points simultaneously.

Before measuring dynamic motions of the test model, static reference data are first obtained by measuring static positions of the targets for 20 s. Next, the model top is excited by an actuator and when a steady state is reached dynamic motions of the model are measured for 100 s that are about ten times the largest natural period of the model. In the data processing facility, a standard software program is equipped to make sampling of model deflections and loads data, to store and to filter digitally in a prescribed way. A graphics window is also provided for on-line observations of the model movements. Sampling rate is 50 Hz for each channel.

Natural Frequency and Mode Shape

The natural frequency of a free hanging marine pipe is dependent on mass, bending stiffness, tension (self-weight) and boundary conditions. In the case of a long flexible pipe, the bending stiffness effect is very small compared to the tension effect. The bending stiffness effect is relevant just in the vicinity of the clamping, within a small boundary layer of order $\sqrt{EI/T}$, EI being the bending stiffness and T the tension at the top. Thorough and enlarged analyses on closed related problems can be found in the literature of Triantafyllou (1984), Irvine (1992), and Aranha et al. (1997).

A closed form solution for mode shapes and natural frequencies of the model without considering a bending stiffness effect can be obtained by employing a Bessel function as follows (Bowman 1958):

$$Z_n(z) = J_0\left(j_{0,n}\sqrt{\frac{z}{L}}\right) \quad (2)$$

where J_n=Bessel Function of the first kind of order zero and $j_{0,n}$=nth zero of $J_n(z)$ and is $j_{0,1}=2.405$, $j_{0,2}=5.52$, $j_{0,3}=8.654$, and $j_{0,4}=11.792$. From Eq. (2), vibration mode shapes of the model can be obtained and are shown in Fig. 2. The natural frequency of the model $\bar{\omega}_n$ and the corresponding natural period T_n can be obtained as follows:

$$\bar{\omega}_n = \frac{2\pi}{T_n} = \frac{1}{2\sqrt{L}} j_{0,n}\sqrt{\frac{g\beta_1}{1+\beta_2}} \quad (3)$$

Using Eq. (3) and data given in Table 1, the first four natural frequencies of the model are calculated and given in Table 2. The first three natural frequencies are $\bar{\omega}_1 = 0.71$ rad/s (8.85 s), $\bar{\omega}_2 = 1.62$ rad/s (3.89 s), and $\bar{\omega}_3 = 2.54$ rad/s (2.47 s).

The natural frequency of the model is also measured at the towing tank experiment to verify the theoretical results. After one large stroke movement at top end, free lateral oscillations of the model are measured. Fig. 3 shows the displacement time history of the model's bottom end where the largest amplitude of the first

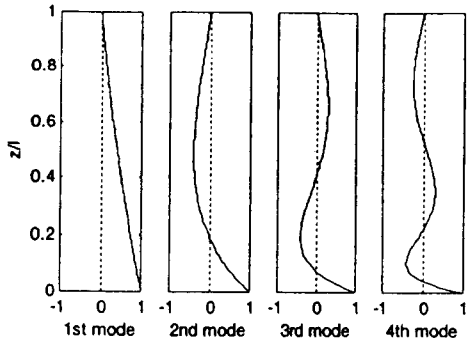

Fig. 2. Vibration mode shape of free hanging model

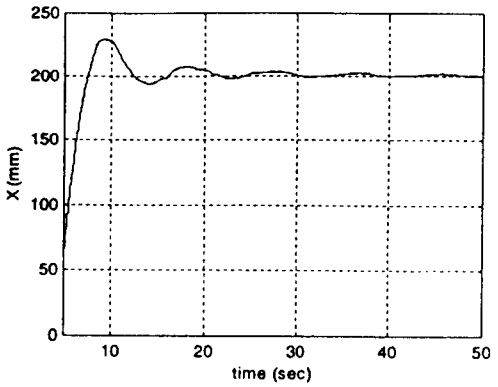

Fig. 3. Measured free vibration

vibration mode occurs. It can be seen from Fig. 3 that the free oscillation dies out quickly due to high fluid damping. The measured natural period is about 9 s and agrees well with the calculated one of 8.85 s by Eq. (3).

Transverse Response to Vortex Shedding

A free hanging immersed model pipe is excited at the top end. Excitation periods are around the first four natural periods and mid natural periods. Two different excitation amplitudes of 100 and 200 mm are used. Even though the model is forced to move in x direction, there are out of plane motions in the y direction, i.e., transverse responses due to vortex shedding. The transverse response plays an important role for the fatigue life of a marine riser or pipe as well as drag forces. In this study, the transverse displacements of the test model are measured and analyzed.

Fig. 4 presents typical time histories of transverse displacements at various points for the excitation amplitude of 100 mm and period of 9 s (close to the fundamental period). In Fig. 4, the uppermost one is the time history of an excitation and ya, yb,...,yi in the vertical axis are transverse displacements at a, b,..., i measuring points. All of the response frequencies are much higher than excitation frequencies. The response frequency is important in transverse responses and thus will be analyzed further in detail in the spectral analysis section. The response amplitude is variant along the model length and largest at the bottom part, as it should be expected.

Fig. 5 shows time histories of transverse displacements at upper, mid, and bottom parts for six excitation frequencies with excitation amplitude of 100 mm. The largest response amplitude occurs at the bottom part for all excitation periods as can be expected. The transversal response frequency seems to increase with the excitation frequency. From Fig. 5, we can see a phenomenon of a low frequency of response oscillation for lower values of excitation periods. It is more evident at a bottom part. This fact indicates that there is a long period of motion with high frequency transverse vibrations. The phenomenon is presumably due to the interaction between in-line and transverse vibrations since it is more evident at the bottom part where larger transverse vibration occurs.

Fig. 6 represents time histories of transverse displacements for the excitation amplitude of 200 mm. The response pattern is similar to the case of the excitation amplitude of 100 mm but the low frequency response oscillation is more evident.

Fig. 7 shows the measured maximum amplitude of transverse vibrations at the upper, mid, and bottom positions of the model plotted against maximum velocity at the top of the model for a wide range of excitation frequencies. It is clearly seen from Fig. 7 that the response amplitude of the bottom part is much larger than upper and mid parts. The amplitude of the mid part is slightly larger than that of the upper part. The response amplitudes of the excitation amplitude of 200 mm (larger in-line motion and thus larger Kc number) are larger than those of the excitation amplitude of 100 mm (smaller in-line motions and thus smaller Kc number). The magnitude of the transverse vibration amplitude of the bottom part is larger than the model diameter but those of mid and upper parts are all smaller than the model diameter.

Table 2. Natural Periods of Test Model by Theory

Mode number	Period(s) [Frequency (rad/s)]
Fundamental	8.85 [0.71]
2nd	3.89 [1.62]
3rd	2.47 [2.54]
4th	1.81 [3.47]
5th	1.43 [4.40]
6th	1.18 [5.33]
7th	1.00 [6.26]

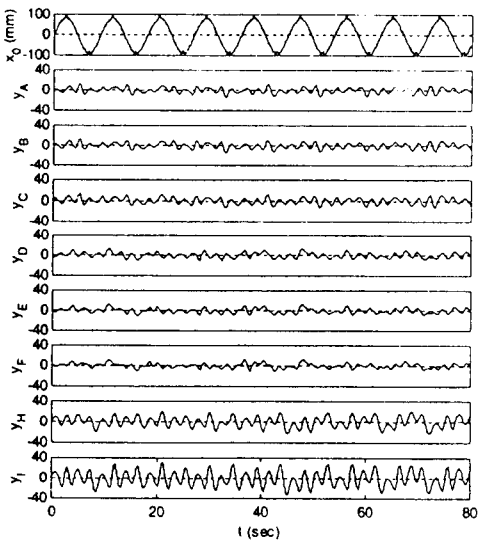

Fig. 4. Time history of measured transverse vibrations of model with excitation period of 9.0 s and amplitude of 100 mm

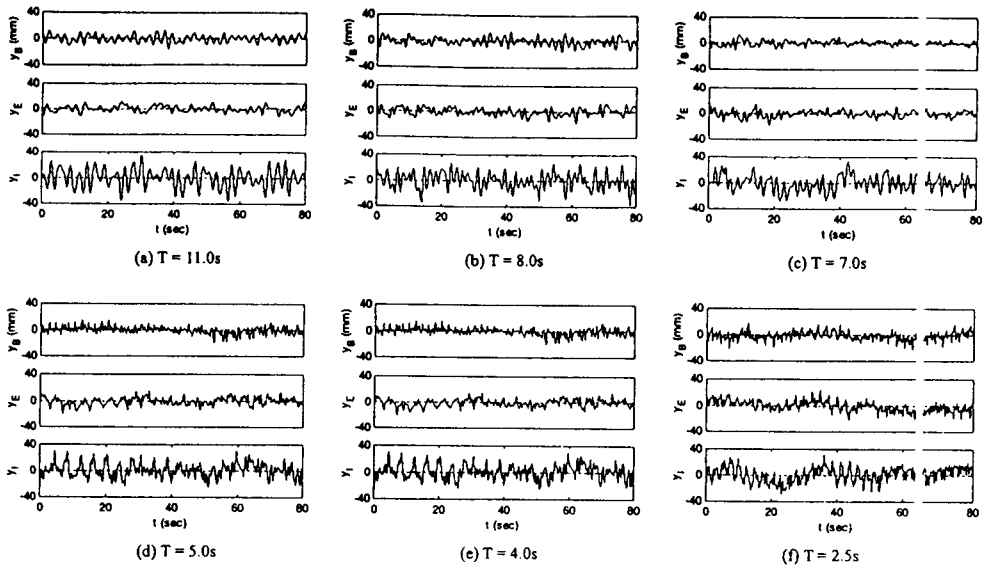

Fig. 5. Time history of transverse vibrations of model with excitation amplitude of 100 mm

Transverse vibrations cause unacceptable levels of fatigue damage to slender marine structures and thus have been studied as an important subject. The fatigue damage is directly connected to response frequencies of transverse vibrations as well as response amplitudes and thus the transverse response frequencies of the test model are examined in detail.

The measured time series data of transverse vibrations are transformed to frequency domain. Fig. 8 represents a typical amplitude spectral density of measured points for an excitation period of 9 s and excitation amplitude of 100 mm. An interesting fact is that a peak commonly exists at the same frequency of 2.76 rad/s (2.28 s) for all measured points. It seems that the peak frequency does not corresponds with any natural frequencies of the model (see Table 2). However, natural frequencies are expected to change as a result of fluid inertia forces as recently observed by many researchers (Leonard and Roshko 2001; Leweke et al. 2001; Vikestad et al. 2000). So, it can be mentioned that the peak frequency is close to the third natural frequency (2.54 rad/s) of the model.

In order to examine this matter, vortex-shedding frequencies of the measured points are determined and compared with the peak frequency of 2.76 rad/s. In order to obtain more exact Kc numbers and thus vortex shedding frequencies at the every measuring point, the inline displacements are also measured. Fig. 9 shows the ratio of response amplitude to excitation amplitude and phase lags between measuring positions for several excitation periods. First the amplitudes of in-line displacements of upper (B point), middle (E point), and bottom (I point) parts are taken from Fig. 9. Then Kc numbers of B,E,I points are, respectively, calculated as 23, 21, and 24 using $Kc=(2\pi A)/D$, where A is the response amplitude in x direction and D is the model diameter. Some researches have been conducted to obtain a relation between Kc

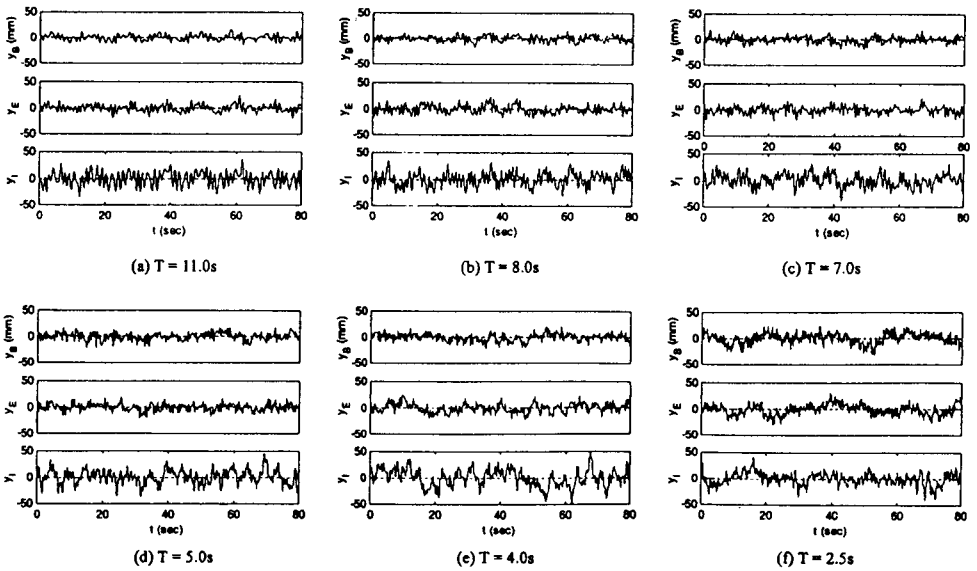

Fig. 6. Time history of transverse vibrations of model with excitation amplitude of 200 mm

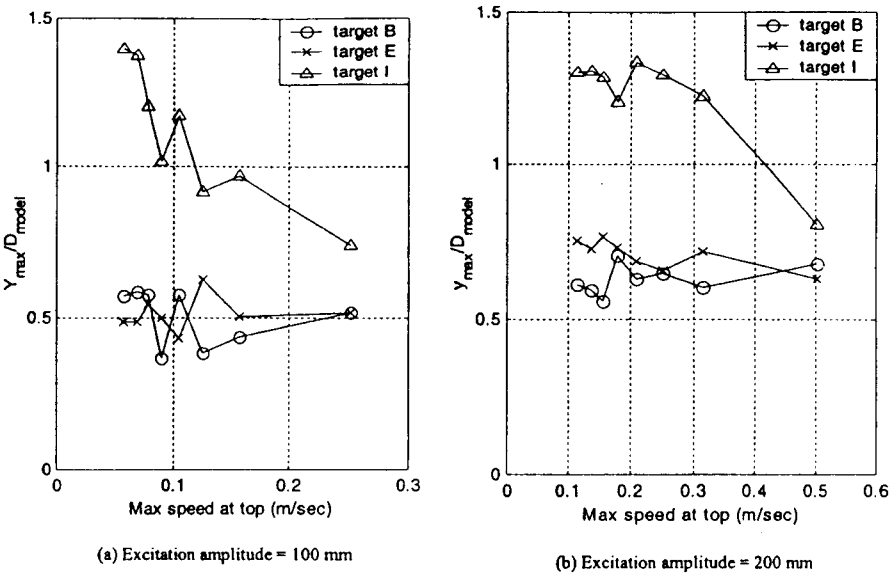

Fig. 7. Maximum amplitudes of transverse vibrations at *B*, *E*, and *I* points

numbers and vortex shedding frequencies of an oscillating slender structure (Koterayama 1984; Blevins 1990). By using the curve of Kc numbers versus vortex shedding frequencies (Koterayama 1984), the corresponding vortex shedding frequencies of *B*,*E*,*I* points are, respectively, obtained as 1.8, 2.1, and 2.8 rad/s. From Fig. 8, we can find that the most dominant peak frequency coincides with vortex shedding frequencies of *B* and *I* points. On the other hand, the response frequency of 2.1 rad/s that is the vortex shedding frequency of *E* point is very week.

The result provides an interesting fact. Even though the vortex shedding frequencies are different according to positions due to the difference of in-line displacements (that is, the difference of Kc numbers), the peak frequencies are all the same at all positions. This is due to the fact that a vortex-induced vibration that happened at a position propagates to other positions and makes the response frequency at other position equal to that of the propagating structural wave. As can be seen from the result of 2.1 rad/s vortex shedding frequency, in this case, a propagating structural wave absorbs other transverse vibrations that occurred at other positions with slightly different frequency.

In order to analyze this fact in more detail, response spectra are obtained for other excitation frequencies (see Fig. 10). Generally, dominant peaks move to high frequency band as excitation frequency increases. For most cases, there are common dominant peaks that occur at the same frequency for the three positions as

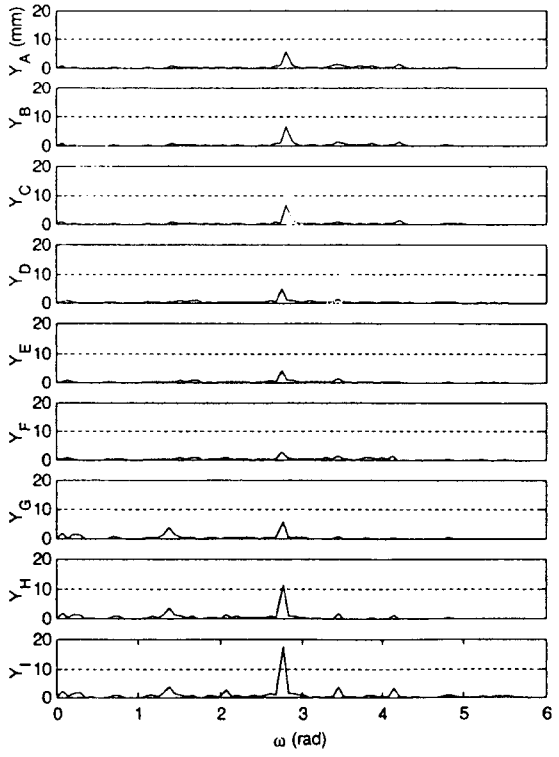

Fig. 8. Response spectrum of measured transverse vibrations of model with excitation period of 9.0 s and amplitude of 100 mm

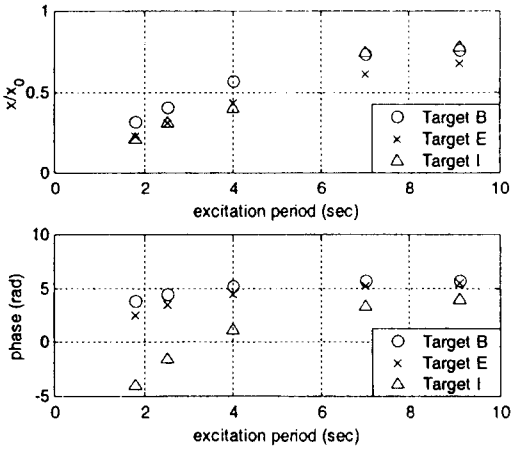

Fig. 9. Maximum lateral displacements and phase difference for different excitation periods (excitation amplitude is 100 mm)

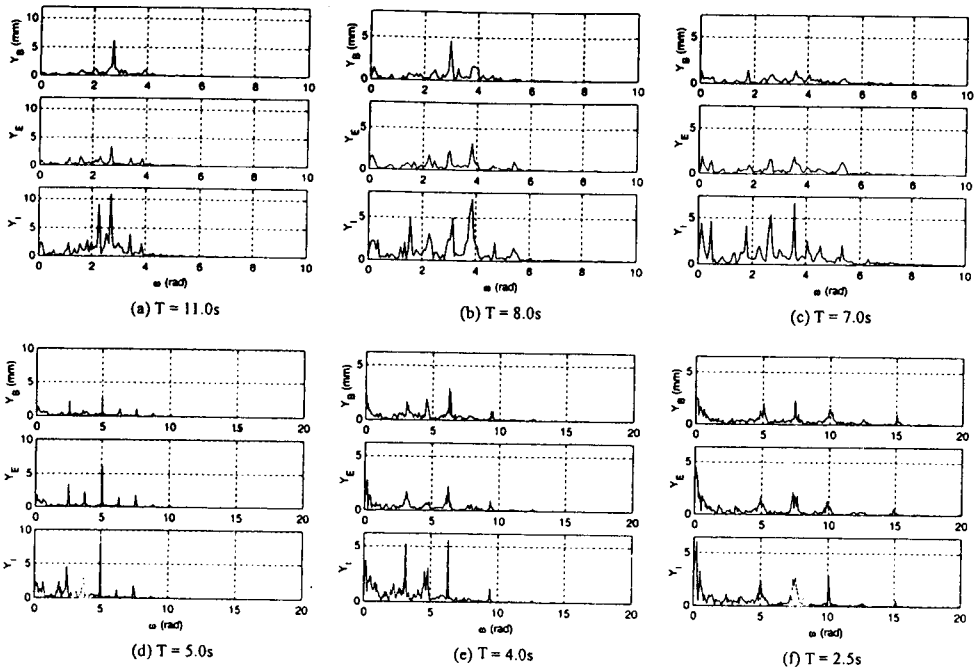

Fig. 10. Response spectrum of measured transverse vibrations of model with excitation amplitude of 100 mm

was in Fig. 8. The vortex shedding frequencies of *B*, *E*, and *I* points are obtained for three excitation frequencies as was done in Fig. 8. Table 3 shows the calculated Kc numbers and vortex shedding frequencies of 9, 7, 4, and 2.5 s excitation periods for the three positions of *B*, *E*, and *I*. Dominant common peak frequencies are also given in Table 3.

By comparing the peak frequencies with vortex shedding frequencies and natural frequencies of the model given in Table 2, we can also find some interesting phenomena as was in 9 s excitation period in Fig. 8. Even though vortex-shedding frequencies are different according to positions, peak frequencies are all the same at all positions. For example, in the case of 7 s excitation period, the vortex shedding frequencies of both *B* and *I* points are 3.6 rad/s and that of *E* point is 2.7 rad/s, but the two frequencies of vibrations simultaneously occur at all positions. As was argued above, this is due to the fact that a particular transverse vibration that occurred at a particular position by a local vortex shedding propagates along the model length as a structural wave.

Concerning the transverse structural wave phenomena, further analysis is necessary. Recently there has been some research on structural wave propagation on marine cables and risers (Behbahani-Nejad and Perkins 1999; Sparks 2001). The celerity of transverse structural wave for a tensioned slender structure can be obtained as follows:

Table 3. Kc Number, Vortex Shedding Frequency, and Dominant Peak Frequency at Measured Positions for Several Excitation Frequencies

Exciting period(s) [frequency(rad/s)]	Point *B* Kc/ω_f	Point *E* Kc/ω_f	Point *I* Kc/ω_f	Peak frequency (rad/s)
9.0 [0.69]	23/2.8	21/2.1	24/2.8	2.76
7.0 [0.9]	24/3.6	19/2.7	24/3.6	3.58,2.68
4.0 [1.57]	18/4.7	13/3.1	12/3.1	6.28,3.14,4.78,
2.5 [2.51]	13/5	9.4/5	9.4/5	10.08,7.56,5.04

$$c = \sqrt{c_t^2 + c_b^2} \tag{4}$$

where c_t and c_b are, respectively, celerity due to tension and bending stiffness effects and they are approximately as follows:

$$c_t = \sqrt{T/m}$$

and

$$c_b = \frac{\pi}{L_n}\sqrt{\frac{EI}{m}} \tag{5}$$

Generally c_b is very small compared to c_t for a deep-sea riser or pipe as was in the natural period case. In the case of a free hanging pipe, structural wave celerity is high in the upper part and low in the lower part because of tension variation. This phenomenon can be easily seen from Fig. 11, where there a numerical simulation of structural wave propagation for 5.03 rad/s frequency and 100 mm amplitude for the model. The result is obtained by using a three dimensional nonlinear finite difference method program developed by the authors (Park and Jung 2002).

It is difficult to clarify transverse structural wave propagation from experimental data because a measured wave data is composed of several different waves and a structural wave varies in time and positions. In this study, an attempt has been made to extract a particular propagating wave from measured wave data. In order to examine the transverse structural wave propagation from a quantitative point of view, the phase lag difference between three continuous points are numerically obtained.

Every response spectrum has one or more peaks. As a case study, a single time history of a peak frequency is extracted from the mixed time series for 9 s excitation period. In that case, the dominant peak occurs at 2.76 rad/s as can be seen from Fig. 8, so a time history of 2.76 rad/s is extracted from Fig. 4 and shown in Fig. 12 for three continuous points of *D*, *E*, and *F*. In numerical values, the phase lag between *D* and *F* points is 0.4387 rad.

The phase lag Δp can be converted to time lag Δt by the following equation:

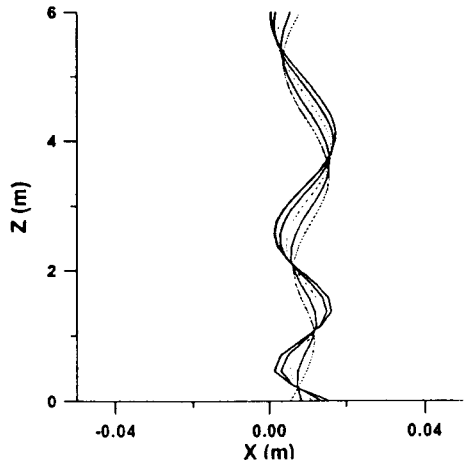

Fig. 11. Numerical simulation of transverse structural wave propagation

$$\Delta t = \Delta p/\omega \tag{6}$$

where ω=peak frequency. Since the peak frequency is 2.76 rad/s and the phase lag is 0.4387 rad, the time lag is 0.159 s.

We have attempted to check and compare the experimental result with a structural wave theory. Since c_b is negligibly small, only c_t is considered in the analysis of the experiment result. At the mid point of the model, the tension is 5.033 N and the total mass per unit length of the model is 0.77 kg/m, so the celerity of transverse structural wave can be calculated as 2.55 m/s by Eq. (5). The time for the wave to propagate from point D to point F can be obtained by dividing the distance between the two points by the celerity. Since the distance is 0.4 m and the celerity is 2.55 m/s, the elapse time is 0.157 s. We can find that the theoretically calculated elapse time, 0.157 s, is nearly equal to the measured time difference, 0.159 s.

This fact indicates that a structural wave initiated at a particular point by vortex shedding propagates along the model length and results in the same frequency of transverse vibrations along the model.

The phenomena of structural wave propagation was also easily observed while carrying out the experiments due to the high flexibility of the model pipe and can be described as follows: when the flexible model is forced to move, vortex shedding occurred first at a position and induced transverse vibrations which propagate down or up along the model length. It looks like a snake movement.

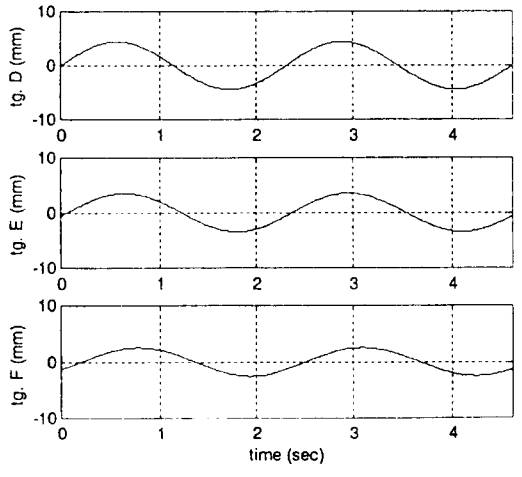

Fig. 12. Example of measured structural wave propagation

Conclusion

Transverse vibrations of a highly flexible free hanging pipe of 6 m in water by top end oscillations are experimentally investigated. For response frequency analyses, natural frequencies of the model are theoretically obtained by considering tension variation along the model length and verified by an experimental result with good agreement. The largest response amplitude of transverse vibrations occurs at the bottom part of the model for all excitation frequencies and amplitudes. Transverse structural wave propagation is observed at the experiment and found in the measured data analysis. A transverse vibration that happened at a position at a vortex shedding frequency propagates to other positions and absorbs other transverse vibrations that occurred at other positions with slightly different frequencies and results in transverse vibrations being the same frequency along the model.

Notation

The following symbols are used in this paper:

A = excitation amplitude;
c_b = celerity due to bending stiffness effect;
c_t = celerity due to tension effect;
D = pipe diameter;
EI = bending stiffness of pipe;
g = gravity acceleration;
J_n = Bessel function of first kind of order zero;
$j_{0,n}$ = nth zero of $J_n(z)$;
k = arbitrary constant;
L = model length;
T = excitation period;
T_n = natural period of model, $n = 1.2.3...$;
w_a = weight per unit length in air;
w_1 = weight per unit length in water;
w_2 = additional weight per unit length due to added mass and internal fluid;
x,y = horizontal coordinates;
z = vertical coordinate;
β_1 = relative weight ($=w_1/w_a$);
β_2 = relative weight ($=w_2/w_a$);
Δp = phase lag of structural wave;
Δt = time lag of structural wave;
Δt_x = time lag error of measured displacement in x direction;
Δt_z = time lag error of measured displacement in z direction;
ω = peak frequency; and
ω_n = natural frequency of model.

References

Aranha, J. A. P., Martins, C. A., and Pesde, C. P. (1997). "Analytical approximation for the dynamic bending moment at the touchdown point of a catenary riser." *Int. J. Offshore Polar Eng.*, 7, 293–300.

Behbahani-Nejad, M., and Perkins, N. C. (1999). "Numerical analysis of nonlinear wave propagation in elastic submerged cables." *J. Offshore Mech. Arct. Eng.*, 121, 116–125.

Blevins, R. D. (1990). *Flow-induced vibration*, Krieger, Malabar, Fla.

Bowman, F. (1958). *Introduction to Bessel functions*, Dover, New York, 25–30.

de Oliveira, M. C., Sphaier, S. H., and Barros, A. M. (2000). "An application of numerical methods to the mechanics of vortex-induced vibrations." *Proc., 10th Int. Offshore and Polar Eng. Conf.*, Vol. 3, Seattle, 511–518.

de Wilde, J. J., and Huijsmans, R. H. M. (2001). "Experiments for high Reynolds numbers VIV on risers." *Proc., 11th Int. Offshore and Polar Eng. Conf.*, Vol. 3, Stavanger, 400–405.

Grant, R., Litton, R., and Finn, L. (2000). "Highly compliant rigid risers: field test benchmarking a time domain VIV algorithm." *Proc., 32nd Offshore Tech. Conf*, Houston, 547–555.

Griffin, O. M., and Ramberg, S. E. (1982). "Some recent studies of vortex shedding with application to marine tubulars and risers." *Am. Soc. Mech. Eng.*, 104, 2–13.

Halse, K. H. (2000). "Norwegian deepwater program: improved predictions of vortex-induced vibrations." *Proc., 32nd Offshore Tech. Conf.*, Houston, 557–564.

Herfjord, K. (1999). "Assessment of vortex-induced vibrations on deepwater risers by considering fluid-structure interaction." *J. Offshore Mech. Arct. Eng.*, 121, 207–212.

Irvine, M. (1992). "Local bending stress in cables." *Proc., 2nd Int. Offshore and Polar Eng. Conf.*, Vol. 2, San Francisco, 342–345.

Kim, W. J., and Perkins, N. C. (2002). "Two-dimensional vortex-induced vibration of cable suspensions." *J. Fluids Struct.*, 16, 229–245.

Koterayama, W. (1984). "Wave forces acting on a vertical circular cylinder with a constant forward velocity." *Ocean Eng.*, 11(4), 363–379.

Leonard, A., and Roshko, A. (2001). "Aspects of flow-induced vibration." *J. Fluids Struct.*, 15, 415–425.

Leweke, T., Bearman, P. W., and Williamson, C. H. K. (2001). "Preface of the special issue on IUTAM Symposium on bluff body wakes and vortex-induced vibrations, BBVIV2, Marseilles, France." *J. Fluids Struct.*, 15, 375–669.

Lyons, G. J., and Patel, M. H. (1986). "A prediction technique for vortex induced transverse response of marine risers and tethers." *J. Sound Vib.*, 111, 467–487.

Moe, G., Holden, K., and Yttervoll, P. O. (1994). "Motion of spring supported cylinders in subcritical and critical water flows." *Proc., 4th Int. Offshore and Polar Eng. Conf.*, Vol. 3, 468–475.

Park, H. I., and Jung, D. H. (2002). "Nonlinear dynamic analysis on low-tension towed cable by finite difference method." *Bull. Soc. Naval Architects Korea*, 39(1), 28–37.

Pesce, C. P., and Fujarra, A. L. C. (1999). "Vortex-induced vibrations and jump phenomenon: experiments with a clamped flexible cylinder in water." *Int. J. Offshore Polar Eng.*, 10(1), 26–33.

Sarpkaya, T. (1979). "Vortex-induced oscillations-a selective review." *J. Appl. Mech.*, 46, 241–258.

Schulz, K. W., and Kallinderis, Y. (2000). "Numerical prediction of the hydrodynamic loads and vortex-induced vibrations of offshore structures." *J. Offshore Mech. Arct. Eng.*, 122, 289–295.

Sparks, C. P. (2001). "Transverse modal vibrations of vertical tensioned risers: a simplified analytical approach." *Proc., 20th Int. Conf. on Offshore Mechanical and Arctic Engineering*, OMAE2001/OFT-1201.

Sumer, B. M., and Fredsoe, J. (1988). "Transverse vibrations of an elastically mounted cylinder exposed to an oscillating flow." *J. Offshore Mech. Arct. Eng.*, 110, 387–394.

Triantafyllou, M. S. (1984). "The dynamics of taut inclined cables." *Q. J. Mech. Appli. Mech.*, 37, 421–440.

Vandiver, J. K., and Li, L. (1997). *SHEAR7 program theoretical manual*, Dept. of Ocean Engineering, Massachusetts Institute of Technology, Cambridge, Mass.

Vikestad, K., and Halse, K. H. (2000). "VIV life coefficients found from response build-up of an elastically mounted dense cylinder." *Proc., 10th Int. Offshore and Polar Eng. Conf.*, Vol. 3, Seattle, 455–460.

Vikestad, K., Vandiver, J. K., and Lasen, C. M. (2000). "Added mass and oscillation frequency for a circular cylinder subjected to vortex-induced vibrations and external disturbance." *J. Fluids Struct.*, 14, 1071–1088.

Whitney, A. K., Chung, J. S., and Yu, P. (1981). "Vibrations of a long marine pipe due to vortex shedding." *J. Energy Resour. Technol.*, 103, 231–236.

Source : Journal of Waterway, Port, Coastal and Ocean Engineering, (2004), 130(4): 207–214